Original Research

Mesenchymal stem cells with p38 mitogen-activated protein kinase interference ameliorate mouse ischemic stroke

Yingying Bai[1] iD, Lishan Wang[2], Rong Xu[1] and Ying Cui[1] iD

[1]Jiangsu Key Laboratory of Molecular and Functional Imaging, Department of Radiology, Zhongda Hospital, Medical School, Southeast University, Nanjing 210009, China; [2]Department of General Surgery, Zhongda Hospital, School of Medicine, Southeast University, Nanjing 210009, China
Corresponding author: Ying Cui. Email: cuiy_seu@163.com

Impact Statement

Factors such as high glucose, oxidative stress, and aging can lead to the reduced function of donor mesenchymal stem cells (MSCs). In this study, we demonstrated that p38 mitogen-activated protein kinase (MAPK) interference in exogenous MSCs by infection with lentivirus could reduce cell senescence and promote the recovery of neurological function and axonal remodeling in stroke mice. This gene-based MSC therapy provides a new potential individualized treatment strategy for ischemic stroke patients, especially for patients with underlying diseases such as diabetes.

Abstract

Mesenchymal stem cells (MSCs) have been widely used in the treatment of ischemic stroke. However, factors such as high glucose, oxidative stress, and aging can lead to the reduced function of donor MSCs. The p38 mitogen-activated protein kinase (MAPK) signaling pathway is associated with various functions, such as cell proliferation, apoptosis, senescence, differentiation, and paracrine secretion. This study examined the hypothesis that the downregulation of p38 MAPK expression in MSCs improves the prognosis of mice with ischemic stroke. Lentiviral vector–mediated short hairpin RNA (shRNA) was constructed to downregulate the expression level of p38 MAPK in mouse bone marrow-derived MSCs. The growth cycle, apoptosis, and senescence of MSCs after infection were examined. A mouse model of ischemic stroke was constructed. After MSC transplantation, the recovery of neurological function in the mice was evaluated. Lentivirus-mediated shRNA significantly downregulated the mRNA and protein expression levels of p38 MAPK. The senescence of MSCs in the p38 MAPK downregulation group was significantly reduced, but the growth cycle and apoptosis did not significantly change. Compared with the control group, the infarct volume was reduced, and the neurological function and the axonal remodeling were improved in mice with ischemic stroke after transplantation of MSCs with downregulated p38 MAPK. Immunohistochemistry confirmed that in the p38 MAPK downregulation group, apoptotic cells were reduced, and the number of neuronal precursors and the formation of white matter myelin were increased. In conclusion, downregulation of p38 MAPK expression in MSCs improves the therapeutic effect in mice with ischemic stroke, an effect that may be related to a reduction in MSC senescence. This method is expected to improve the efficacy of MSCs in patients, especially in patients with underlying diseases such as diabetes, thus providing a basis for clinical individualized treatment for cerebral infarction.

Keywords: Mesenchymal stem cells, stem cell therapy, p38 MAPK, ischemic stroke, diffusion tensor imaging, magnetic resonance imaging

Introduction

Ischemic stroke has a high incidence, high prevalence, and high recurrence rate, with a poor prognosis and extremely high disability and mortality rates. For many patients outside the therapeutic time window of thrombolytic therapy, the repair of neurological damage after stroke is extremely important. Mesenchymal stem cells (MSCs) are mesodermal cells that can be obtained from a variety of sources, such as adipose tissue, bone marrow (BM), and umbilical cord blood. Through many animal and clinical studies, MSCs have been confirmed to have good safety and neuroprotective effects after cerebral infarction. MSCs can effectively reduce inflammation, regulate immune responses, inhibit neuronal apoptosis, promote angiogenesis and fiber regeneration, thereby accelerating the recovery of neurological function and improving prognosis.[1,2] In addition, the effect of BM-derived MSCs is superior to that of umbilical cord blood- and adipose tissue-derived MSCs. In addition to homing to the injury site, MSCs can not only differentiate into neurons, glial cells, and endothelial cells but also promote the repair of neurological damage through the secretion of trophic factors by exosomes

next to the injured environment.[3] After the *in vitro* labeling of MSC exosomes, we dynamically monitored the homing process of exosomes to the cerebral infarction site *in vivo* and observed their neuroprotective effects.[4] However, the application of MSCs is complicated by certain donor factors, such as old age and underlying diseases.[5] Factors such as high glucose, oxidative stress, and aging can cause MSCs to undergo senescence and apoptosis, thus hindering cell expansion and reducing paracrine secretion; therefore, the therapeutic potential of autologous MSCs in these patients is significantly reduced.[5] It is thus necessary to develop effective methods to improve cell function and improve the efficacy of cerebral infarction treatment. We believe that the targeted regulation of senescence signaling pathways in MSCs may be an effective strategy to rejuvenate MSCs.

p38 mitogen-activated protein kinase (MAPK) belongs to the family of mitogen-activated protein kinases, is a key kinase that promotes proliferation and transmits stress signals in cells, and is a key regulator of several cellular physiological processes including proliferation, apoptosis, senescence, differentiation, and paracrine secretion.[6] The p38 MAPK signaling pathway is closely related to various influencing factors, such as hyperglycemia, endothelial nitric oxide synthase/nitric oxide (eNOS/NO), and oxidative stress.[7,8] p38 MAPK gene interference has been reported to effectively inhibit high glucose-induced osteoblast apoptosis[9] and aldosterone-induced cardiomyocyte apoptosis.[10] A p38 MAPK-specific inhibitor has been shown to not only significantly inhibit the senescence of MSCs during viral transduction and improve their proliferation and differentiation[11] but also improve the hematopoietic function of hematopoietic stem cells and the angiogenic function of endothelial progenitor cells in a stressful or high-glucose environment.[6,12] These studies emphasized the cell-autonomous role of p38 MAPK signaling in stem cells; however, there is no report indicating the role of the regulation of p38 MAPK signaling, which is ubiquitous in stromal cells, in the treatment of ischemic stroke by MSCs.

p38 MAPK is widely present in various tissues and cells in the body. The systemic inhibitor would inevitably affect the normal physiological processes of other tissues and cells. The production of cytokines in cerebral ischemia/reperfusion injury is also closely related to the p38 MAPK pathway. The use of inhibitors in the early stage of cerebral infarction can significantly inhibit neutrophil chemotaxis and superoxide production, reduce inflammatory responses, and improve patient prognosis.[13] However, the inflammatory response plays a double-edged role in the course of cerebral infarction.[14] In the early stage, the inflammatory response can aggravate ischemic brain injury, but in the later stage, it can remove cell debris associated with necrotic brain tissue and degrade the extracellular matrix, thereby promoting angiogenesis and neurogenesis. The long-term use of p38 MAPK inhibitors may simultaneously inhibit the two-sided effects of inflammatory responses. In addition, the dose of such inhibitors is also difficult to control, the inhibitory effect of small doses is poor, the maintenance time of the plasma concentration is limited, thus not allowing continuous improvements in the working environment of exogenous MSCs; while large doses will inhibit the activities of other upstream and downstream kinases.

Therefore, in this study, we test the hypothesis that the expression of p38 MAPK in exogenous MSCs can be down-regulated in a long-term, high-efficiency, specific and stable manner through the use of RNA interference (RNAi) technology. The effect of stem cell treatment was dynamically evaluated from the aspects of infarct volume and the integrity of white matter fiber tracts via magnetic resonance imaging (MRI).

Materials and methods

Cell culture

C57BL/6 mouse BM-derived MSCs were purchased from Cyagen Biosciences (Guangzhou, China).[4] The cells were seeded into six-well plates (Corning, Corning, NY, USA) in a single-cell suspension. Approximately $(2.5-3.5) \times 10^5$ cells in 2 mL of complete medium were seeded in each well. The medium was Dulbecco's modified Eagle's medium (DMEM)/F12 (Hyclone, Logan, UT, USA) supplemented with 10% fetal bovine serum (FBS) (Gibco, Paisley, UK), and the cells were cultured in an incubator at 37°C with 5% CO_2 and saturated humidity.

Lentiviral vectors production and infection of MSCs

The construction and preparation of lentiviral vectors were completed by Cyagen Biosciences (Guangzhou, China). RNAi sequence design software was used to design three RNAi target sequences about the target gene p38 MAPK, and the target sequence with the highest interference efficiency (CCAACAATTCTGCTCTGGTTA) was selected to synthesize the lentiviral vector p38-short hairpin RNA (shRNA) containing enhanced green fluorescent protein (*eGFP*) gene. A negative control viral vector only containing *eGFP* gene, that is, NC-shRNA (TTCTCCGAACGTGTCACGT), was randomly selected. Using Lipofectamine 2000 (Invitrogen, Carlsbad, CA, USA), the lentiviral vector and the packaging plasmid ViraPower™ Lentiviral Packaging Mix (Invitrogen) were co-transfected into 293FT cells for amplification. After 48 h, the virus-containing supernatant was collected and centrifuged at 3000 r/min for 15 min at 4°C to remove cell debris. After filtration through a 0.45-micron filter, supernatant rich in lentiviral particles was collected and concentrated for later use. The tenth echelon dilution method was used to measure the infective viral titer. Briefly, HEK293T cells were plated in a 96-well plate at a density of 2×10^4 cells/100 μL in each well, and infected with a serial dilution of lentiviral vectors. Culture media were replaced with fresh media 6 h after infection, and the number of fluorescent cells in each well was determined 96 h after infection. The final infection titer of the lentiviral particles was 10^8 transducing units (TU)/mL.

Third-generation MSCs with a good growth status and appropriate cell density (30–50% confluence) were selected. The original medium was removed from the cells and replaced with fresh complete medium. The cells were placed in an incubator to equilibrate before transfection. The cells

were randomly divided into two groups, that is, gene knock-down group (p38-shRNA group) and negative control group (NC-shRNA group), which were stably transfected with lentiviral p38 MAPK-shRNA or control lentiviral shRNA, respectively. Cells were transferred to serum-free media containing 5 mg/mL polybrene (Sigma-Aldrich, St. Louis, MO, USA) and lentiviral particles at multiplicity of infection (MOI) of 30. The cells were cultured in an incubator for 12 h, and the medium was replaced with fresh complete medium. Cells were passaged after 72 h of infection. Infection efficiency was determined based on the expression of green fluorescent protein (GFP) in the cells observed by an inverted fluorescence microscope (Carl Zeiss, Jena, Germany).

Reverse transcription–quantitative polymerase chain reaction and western blot

Reverse transcription–quantitative polymerase chain reaction (RT-qPCR) was performed to determine the level of p38 MAPK mRNA expression. Total RNA was extracted using a kit (Takara, Japan). Reverse transcription was performed using a Takara PrimeScript RT reagent kit with gDNA Eraser (Perfect Real Time). The human GAPDH (*hGAPDH*) gene was used as an internal control to quantitatively analyze the relative expression of the target gene in samples. Three replicate wells were analyzed for each sample, and the relative quantification was performed using the $2^{-\triangle\triangle Ct}$ method.

Western blot was performed to determine the level of p38 MAPK protein expression. Cells were lysed with radio-immunoprecipitation assay (RIPA) lysis buffer (Beyotime, China), and 30 μg of total protein was used for Western blot analysis. The proteins were separated in a 12% separation gel and then transferred (wet transfer at 300 mA for 70 min) to a membrane, which was blocked in 5% non-fat milk for 1 h. The membranes were then incubated with rabbit anti-mouse p38 MAPK primary antibody (1:1000, Cell signaling Technology, Danvers, MA, USA) and GAPDH antibody (1:2000, Abcam, Cambridge, MA, USA) at 4°C overnight. Then, the membranes were incubated with horseradish peroxidase (HRP)–conjugated goat antirabbit secondary antibody (1:1000, Life Technologies, The Netherlands) for 1.5 h at room temperature. Images were analyzed using ImageJ analysis software.

Fluorescence-activated cell sorting

MSCs survival after infection was determined through cell cycle and cell apoptosis analyses by fluorescence-activated cell sorting (FACS). MSCs with good condition after infection were selected and cultured for 48 h. The cells were harvested by trypsin digestion and washed twice with phosphate-buffered saline (PBS) and fixed with 70% ice cold ethanol at 4°C overnight, followed by treatment with povidone-iodine (PI, Sigma-Aldrich) solution at a final concentration of 50 μg/mL. Cellular DNA content was detected with FACS and cell cycle analysis was performed with BD FACSDiva™ software.

For detection of cell apoptosis, an Annexin V-APC/PI detection kit (Elabscience, China) was used according to the manufacturer's instructions. The cells were suspended in 400 μL of Annexin V binding solution at a concentration of approximately 1×10^6 cells/mL. Then, 5 μL of Annexin V-APC staining solution was added to the cell suspension, and the solution was gently mixed and incubated at 4°C in the dark for 15 min. After adding 10 μL of PI staining solution, the cell suspension was gently mixed and incubated at 4°C in the dark for 5 min. Within 1 h, the percentage of early apoptotic cells was determined with FACS.

β-galactosidase staining of MSCs

MSCs with good condition after infection were selected and cultured for four days. For β-galactosidase staining, 1 mL of fixation solution was added to the cells after washing with PBS once, followed by fixation at room temperature for 15 min. Subsequently, the cell fixation solution was removed, and the cells were washed with PBS 3 times (3 min each). The staining solution was prepared following the instructions provided with the kit (Beyotime, China). After the PBS was removed, 1 mL of the staining solution was added to each well, the six-well plate was sealed with a plastic wrap to prevent evaporation, and the cells were incubated at 37°C overnight. Cell senescence was observed under an inverted microscope.

Animal model

All animal experiments were approved by the Institutional Animal Care and Use Committee of the Medical School of Southeast University (SYXK 2021-0022). C57BL/6J mice (25–27 g, 8–10 weeks, male) were adapted to the experimental conditions for seven days before experimentation. A focal cerebral infarction mouse model was established using the photochemical method. Mice were maintained under anesthesia with 1.0% isoflurane. After the scalp of the mice was depilated, the mice were fixed in the prone position, rhodamine (100 mg/kg) was injected intraperitoneally, and a cold light (4 mm diameter) was then centered 2.0 mm to the right of the bregma for 15 min. Twenty-four hours later, successful modeling was determined using T2-weighted imaging (T2WI).

After another 24 h, the mice were randomly divided into two groups, followed by intracardiac injection of MSCs transfected with lentiviral p38 MAPK-shRNA or control lentiviral shRNA, respectively. Approximately 150 μL of MSC suspension (containing 10^6 cells) was injected slowly into the left ventricle. After the injection, the mice were kept warm until they were fully awake and were then returned to their cages.

Neurological function scores

On the 14th day after MSC injection, the mice in each group were assessed using the modified neurological severity score (mNSS) and the foot-fault test to evaluate behavioral functions. The mNSS score reflected the severity of nerve damage in the mice. This score was determined by motor, sensory, reflex, and balance tests with scores ranging from 0 to 18 (Supplemental Material). Higher test scores indicated more severe neurological deficits.[15] In the foot-fault test, mice were placed on a wire mesh (the length and width of each cell was 1 cm), and a camera recorded the number of times mice stepped into the mesh with their left forelimb and the number of all steps in 5 min, allowing the calculation of a

percentage of steps in the mesh. There were six to eight mice in each group, and scoring was performed by an experimenter who blinded to the grouping.

MRI and quantification

MRI was performed using a 7.0 T small animal magnetic resonance scanner (Bruker PharmaScan, Ettlingen, Germany). T2-weighted imaging (T2WI) and diffusion tensor imaging (DTI) were used to evaluate the infarct volume and white matter fiber tract remodeling. Inhalation anesthesia was used during the MRI scan. The induction dose of isoflurane mixed with oxygen was 5%, and the maintenance dose was 1%. Model mice were placed in prone position with the head in the center of the surface coil, and the head of the mouse was fixed. Respiratory rhythm and amplitude were monitored, the dose of anesthetic was adjusted to keep the respiratory rate at 25–35 breaths per minute, and a water system was used to keep the mice warm.

T2WI was acquired using a relaxation enhanced rapid acquisition sequence. The scanning parameters are as following: repetition time (TR) = 3000 ms; echo time (TE) = 36 ms; field of view (FOV) = 2 cm × 2 cm; matrix = 256 × 256; flip angle = 180°; number of excitations (NEX) = 2; number of slices = 12; slice thickness = 1 mm. T2WI was scanned before and on day 21 after MSC injection, with five to six animals in each group. The images were analyzed using ImageJ software. The volumes of the infarcted area and the contralateral brain tissue were delineated and calculated, and the difference in volume percentage of the infarcted lesion to the contralateral brain tissue between day 0 and day 21 was calculated.

DTI was acquired using an echo planar imaging sequence. The scanning parameters are as following: TR = 5000 ms; TE = 32.2 ms; b value = 0 and 1000 s/mm^2; FOV = 1.6 cm × 1.6 cm; matrix = 128 × 128; NEX = 2; number of slices = 12; slice thickness = 0.6 mm; 30 distinct diffusion directions and five reference images. DTI was scanned on day 21 after MSC injection, with five to six animals in each group. Image analyses and data measurements were performed using the ParaVision 5.0 software (Bruker PharmaScan MRI). A tensor map was created from the images, and the fractional anisotropy (FA) of the internal capsule (IC) on the right side of the brain was calculated. Fiber tracking was performed using the TrackVis (version 0.5.2.1; Massachusetts General Hospital, Boston, MA, USA) and Diffusion Toolkit (version 0.6.2.1; Massachusetts General Hospital) software.

Immunohistochemistry

On day 21, the animal brains were dissected and embedded in paraffin or optimum cutting temperature (OCT) compound.

The paraffin-embedded brains were sectioned into 4 μm slices and incubated with a rabbit polyclonal antimyelin basic protein (MBP) antibody (Abcam, Cambridge, UK) at 4°C. Then, the slices were examined under a microscope (Zeiss, Germany).

The OCT-embedded brains were cryostat-sectioned into 10 μm and incubated with rat monoclonal anti-BrdU (Abcam, USA), and rabbit anti-Dcx (Abcam, USA) antibodies followed by staining with secondary Alexa Fluor antibodies (Thermo Fisher Scientific, Waltham, MA, USA), including goat anti-rabbit 488 and goat antirat TRITC. In addition, a terminal transferase–mediated dUTP nick-end labeling (TUNEL) assay was performed using an *In Situ* Cell Death Detection Kit Fluorescein (Roche, Indianapolis, IN, USA) to measure neuronal cell death. These sections were scanned by confocal microscopy (Olympus, LEXT, Japan). Quantification was performed by an investigator blinded to the experimental groups.

Statistics

The SPSS software, version 18, was used to process all experimental data. Numerical data are expressed as the mean ± SD. For statistical comparisons, the independent sample t-test was used to compare the means between two groups. A P value of less than 0.05 was considered statistically significant.

Results

Infectivity of lentiviruses in MSCs

The infectivity of viral preparations was tested on MSCs. Immunocytochemistry indicates that more than 80% of MSCs were GFP positive in the p38 MAPK-shRNA group and the NC-shRNA group after infection (Figure 1(a)), and the cells were in good condition, indicating acceptable transfection efficiency.

Lentiviral p38 MAPK-shRNA infection downregulates mRNA and protein expression levels of p38 MAPK in MSCs

The level of p38 MAPK mRNA expression in the p38-shRNA group was significantly downregulated, that is, 27.67 ± 5.67% of that in the control group (Figure 1(b), $P < 0.01$). In addition, compared with that in the NC-shRNA group, the level of p38 MAPK protein expression in the p38-shRNA group was also significantly lower (Figure 1(c), $P < 0.01$), indicating successful p38 MAPK interference of MSCs.

Downregulation of p38 MAPK does not affect the cell cycle and cellular apoptosis of MSCs

Compared with those in the NC-shRNA group, the percentages of cells in the G1, S, and G2 phases in the p38-shRNA group did not change significantly (Figure 2(a) and (b), $P > 0.05$). In addition, there was no significant difference in the percentage of early apoptotic cells between the p38-shRNA group and the NC-shRNA group (Figure 2(c) and (d), $P > 0.05$).

Downregulation of p38 MAPK decreases cellular senescence in MSCs

Compared with that in the NC-shRNA group, the number of senescent MSCs in the p38-shRNA group was significantly lower (Figure 3(a)), and there was a significant difference between the two groups (Figure 3(b), $P < 0.01$). These results suggest that treatment of MSCs with p38 MAPK interference could reduce cellular senescence, which may further
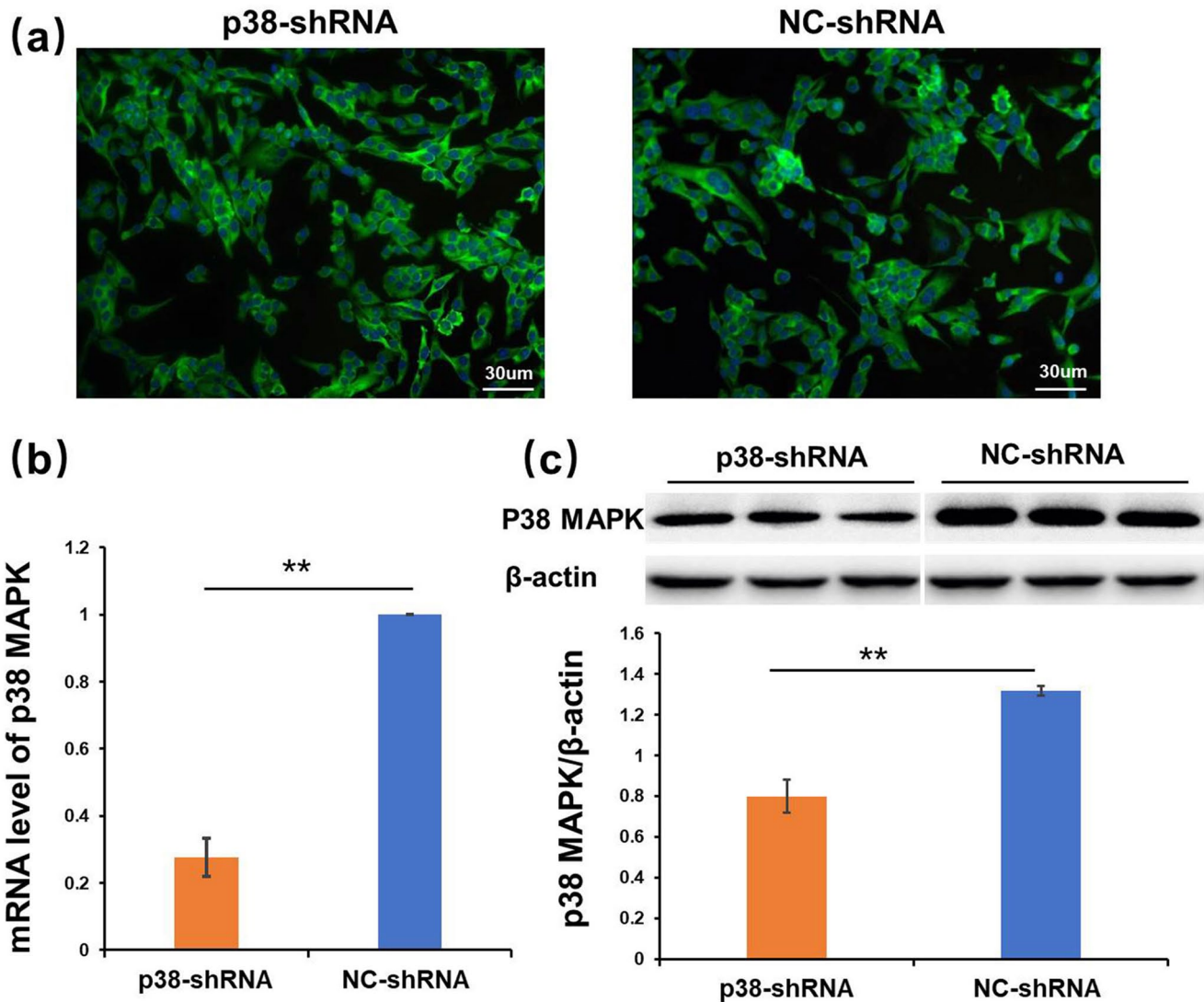
Figure 1. Infectivity of lentiviruses in mesenchymal stem cells (MSCs). (a) Representative fluorescent microscopy images illustrated the expression of GFP in MSCs infected with lentivirus (scale bar = 30 μm). Quantitative analysis of the level of p38 MAPK mRNA (b) and protein expression (c) in MSCs after lentiviral transfection. **$P < 0.01$.

enhance the biological function and then improve the therapeutic effect of MSCs.

MSCs infected with p38-shRNA promote the recovery of neurological function and a reduction in infarct volume in mice

The successful rate of mouse modeling was approximately 95%, and the mice without lesions in the brain confirmed by T2-weighted MRI were excluded from the experiments. All selected animals were in good condition. Two groups of MSC-transplanted mice were subjected to mNSS assessments (Figure 4(a)) and foot-fault tests (Figure 4(b)) on day 14 after MSC injection to score their neurological deficits. MSC transplantation in the p38-shRNA group significantly reduced the behavioral deficits in mice on day 14 (Figure 4(a) and (b), $P < 0.05$).

Representative T2-weighted images of MSC-transplanted mice on day 21 in two groups are shown in Figure 4(c). The difference in the size of the cerebral infarction lesion at day

0 and day 21 in each group was compared, and the results indicated that compared with that in the NC-shRNA group, the difference in the infarction volume before and after MSC transplantation in the p38-shRNA group significantly increased (Figure 4(d), $P < 0.05$), indicating that the infarction volume significantly decreased and that the treatment effect was significant.

MSCs infected with p38-shRNA increase axonal remodeling in mice

In vivo DTI was performed to evaluate the integrity of white matter fibers in the brains of mice in each group on day 21 after MSC injection. Region of interest (ROI) was set at the bilateral internal capsule (Figure 5(a)). DTI reconstruction showed that the corticospinal tract on the right side showed continuity interruption and loss of anatomical structure morphology (Figure 5(a)) and that MSC transplantation in the p38-shRNA group significantly increased the FA value (Figure 5(b), $P < 0.05$) and the number and length of fiber
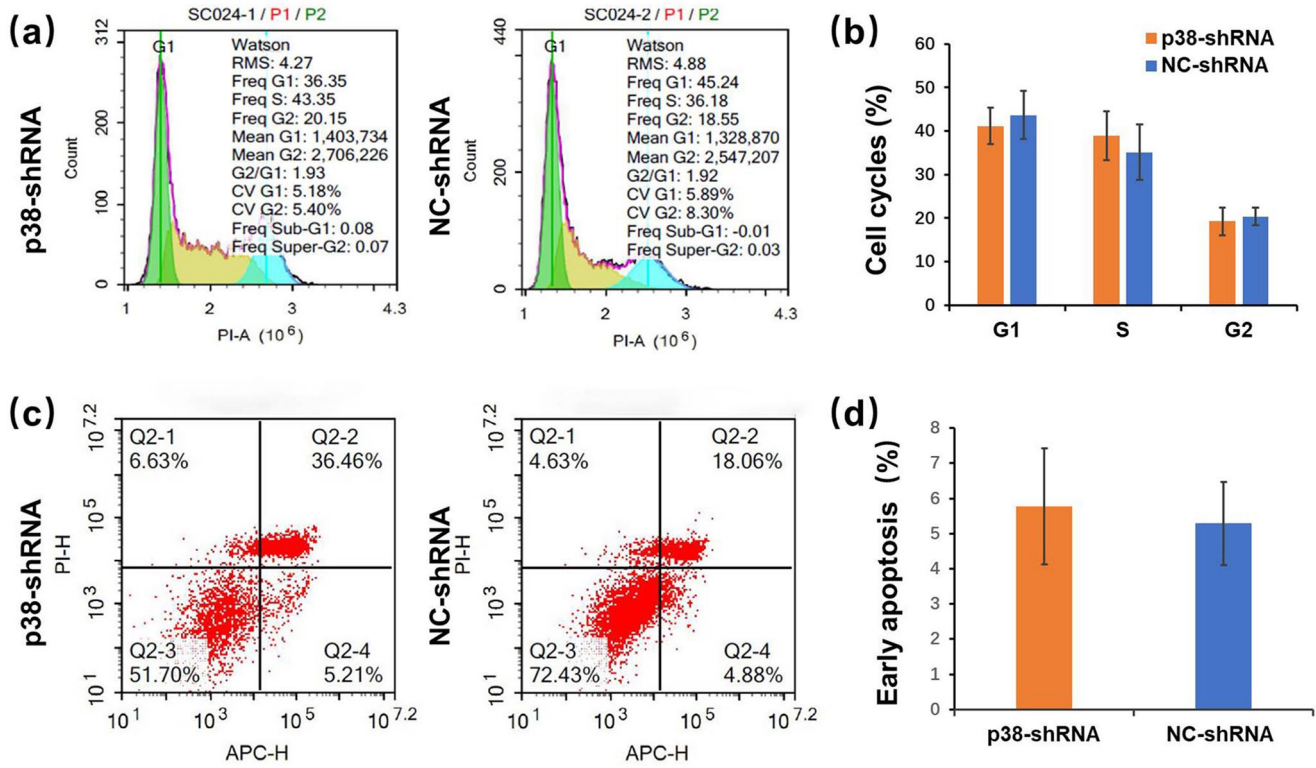
Figure 2. Downregulation of p38 MAPK does not affect the cell cycle or cellular apoptosis of mesenchymal stem cells (MSCs). (a) Representative images of the cell cycle analyzed by FACS are shown in the upper panel. (b) DNA content during different periods of the cell cycle indicated that there was no significant difference between p38-shRNA infected MSCs and NC-shRNA-infected MSCs. (c) Representative images of cell apoptosis analyzed by FACS are shown in the lower panel. Early apoptosis is shown in the right lower quadrant. (d) No significant difference was observed in early apoptosis analyses between the two different groups. $P > 0.05$. Cell cycle and apoptosis experiments indicated that downregulation of p38 MAPK does not affect the cell cycle or cellular apoptosis of MSCs.
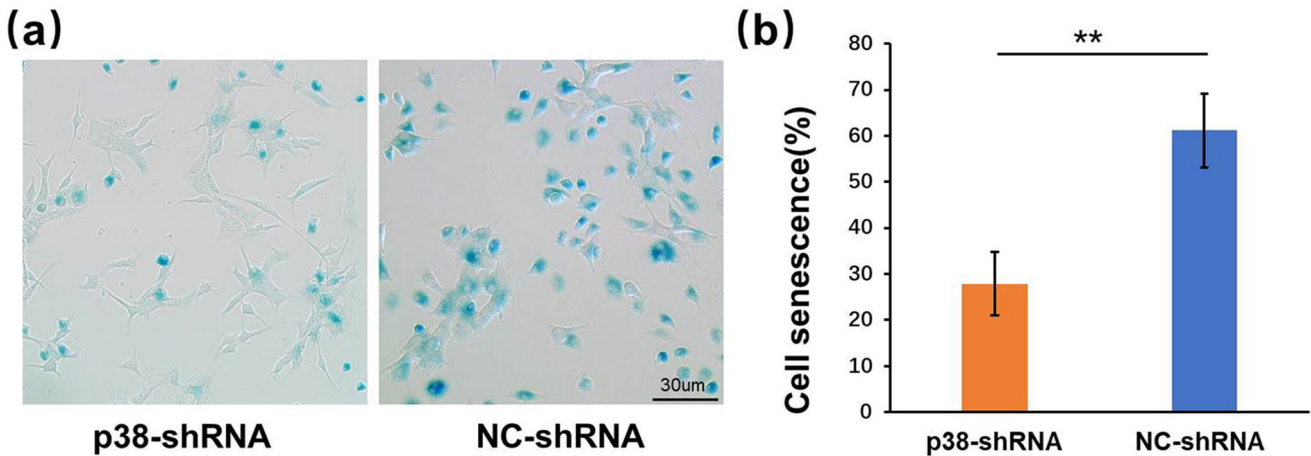

Figure 3. Downregulation of p38 MAPK decreases cellular senescence in mesenchymal stem cells (MSCs). (a) Senescence-associated β-galactosidase staining assays of MSCs in two different groups are shown. Senescent cells exhibit high expression of SA-β-gal in blue staining (scale bar = 30 μm). (b) Quantitative analysis of the number of senescent MSCs showed significant differences between the two groups (**$P < 0.01$), indicating that downregulation of p38 MAPK decreases cellular senescence in MSCs.

tracts (Figure 5(c) and (d), $P < 0.05$) in the ipsilateral internal capsule.

Immunohistochemical staining (Figure 5(e)) also showed that in the p38-shRNA group, the number of MBP-positive cells in the ipsilateral internal capsule significantly increased (Figure 5(f), $P < 0.05$), indicating that the damage on the myelin of the internal capsule improved significantly.

MSCs infected with p38-shRNA promote neurogenesis and decrease apoptosis in mice

On day 21 after MSC injection, brain tissue was frozen and sectioned, and apoptotic cells at the edge of the lesion (black frame, Figure 6(a)) and proliferating neural precursor cells in the ipsilateral subventricular zone (red frame, Figure 6(a)) were determined. Compared with MSC transplantation in
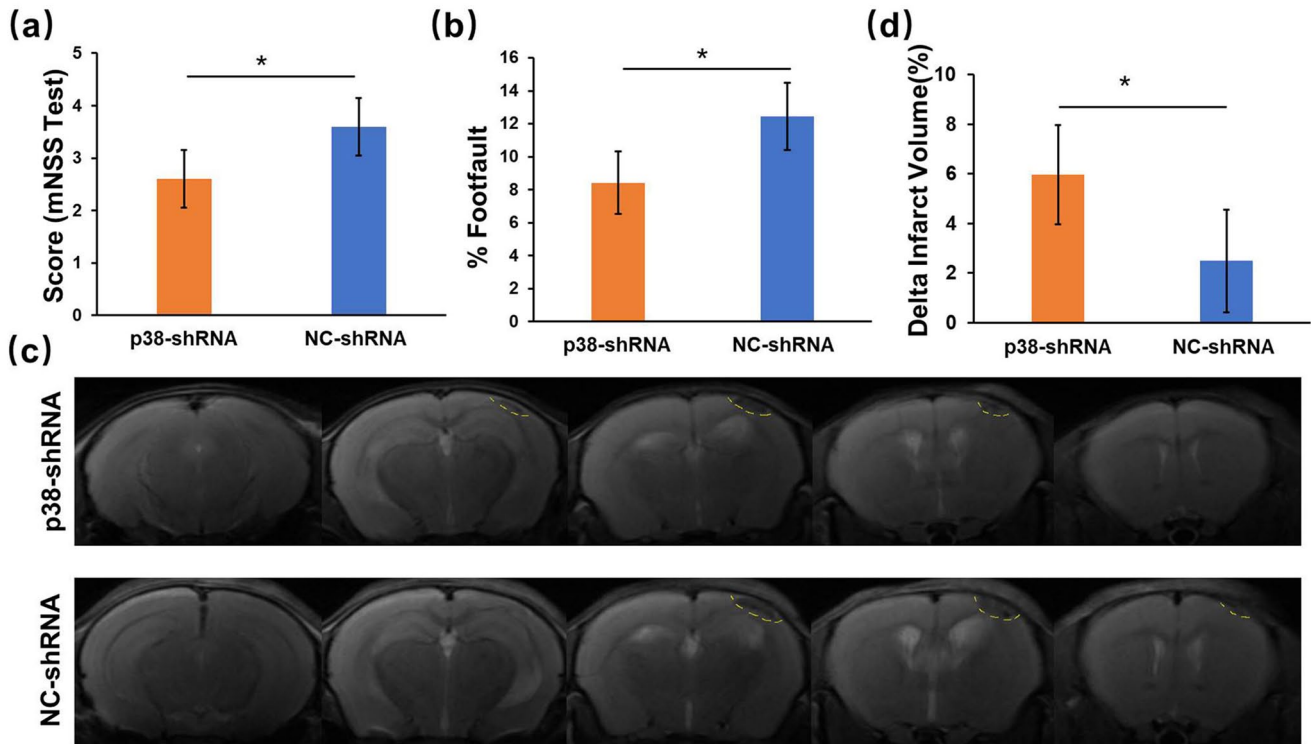
Figure 4. Mesenchymal stem cells (MSCs) infected with p38 MAPK-shRNA promote the recovery of neurological function and a reduction in infarct volume in mice. Quantitative analysis of modified neurological severity score (mNSS) analysis (a) and foot-fault tests (b) in mice of two groups on day 14 (*$P < 0.05$). (c) Representative T2-weighted images of MSC-transplanted mice in two groups on day 21 are shown in the lower panel. Infarct regions are outlined by yellow dotted line. (d) Quantitative analysis of delta infarct volume, that is, the difference in the infarction volume at day 0 and day 21 showed a significant reduction in infarct volume in mice treated with p38 MAPK-shRNA infected MSCs (*$P < 0.05$).

the NC-shRNA group, MSC transplantation in the p38-shRNA group significantly reduced the number of apoptotic cells at the edge of the infarct (Figure 6(b) and (c), $P < 0.01$) and significantly increased the number of BrdU/Dcx double-positive cells in the subventricular zone (Figure 6(d) and (e), $P < 0.05$), indicating that MSC transplantation combined with p38MAPK interference reduced cell apoptosis at the edge of the lesion and promoted neurogenesis in the subventricular zone after stroke in mice.

Discussion

The results of this study indicated that the inhibition of p38 MAPK signaling in MSCs could reduce cell senescence, enhance function, and improve the efficacy of stroke treatment.

MSCs can differentiate into chondrocytes, adipocytes, and osteoblasts and can transdifferentiate into endothelial cells, glial cells, and neurons. Because BM-MSCs are easy to isolate and expand, the risk of immune rejection in allogeneic transplantation is relatively low, and thus, they are the main source of cell therapy for many diseases. More than 700 clinical trials have been registered.[16] There are two mechanisms by which BM-MSCs effectively treat stroke: at the peripheral level, with a reduction in inflammatory response and immune regulation, and at the central level, with effects on angiogenesis, neurogenesis, astrocytes, axons, and oligodendrocytes.

However, due to the limited number of available cells, the use of BM-MSCs is limited. Therefore, to become a clinical option, BM-MSCs must undergo several *in vitro* expansions to obtain sufficient cell numbers for immediate application, a process that leads to another bottleneck, that is, the replicative senescence or premature senescence of BM-MSCs.[17] Regardless of the age of the donor, BM-MSCs inevitably acquire a senescent phenotype after long-term *in vitro* expansion, further hindering their long-term function. Even limited *in vitro* passage can lead to the rapid aging of MSCs, which is characterized by excessive reactive oxygen species (ROS) production and a transition to adipogenic differentiation.[18–20] The premature senescence of *in vitro* cultured BM-MSCs is associated with oxidative stress. The increase in oxidative stress leads to the loss of stem cell characteristics and the destruction of the self-renewal and differentiation ability of MSCs, which has a significant impact on their therapeutic potential.[18] In addition, factors such as high glucose can also lead to cell senescence, with the main causative factors being mitochondrial dysfunction and oxidative stress.[21] High levels of glucose enhance mitochondrial metabolism and induce mitochondrial ROS production through the tricarboxylic acid cycle and oxidative phosphorylation.[22] Cell senescence induced by these stress-related factors can reduce the efficacy of transplanted BM-MSCs in tissue regeneration and the treatment of autoimmune and inflammatory diseases.

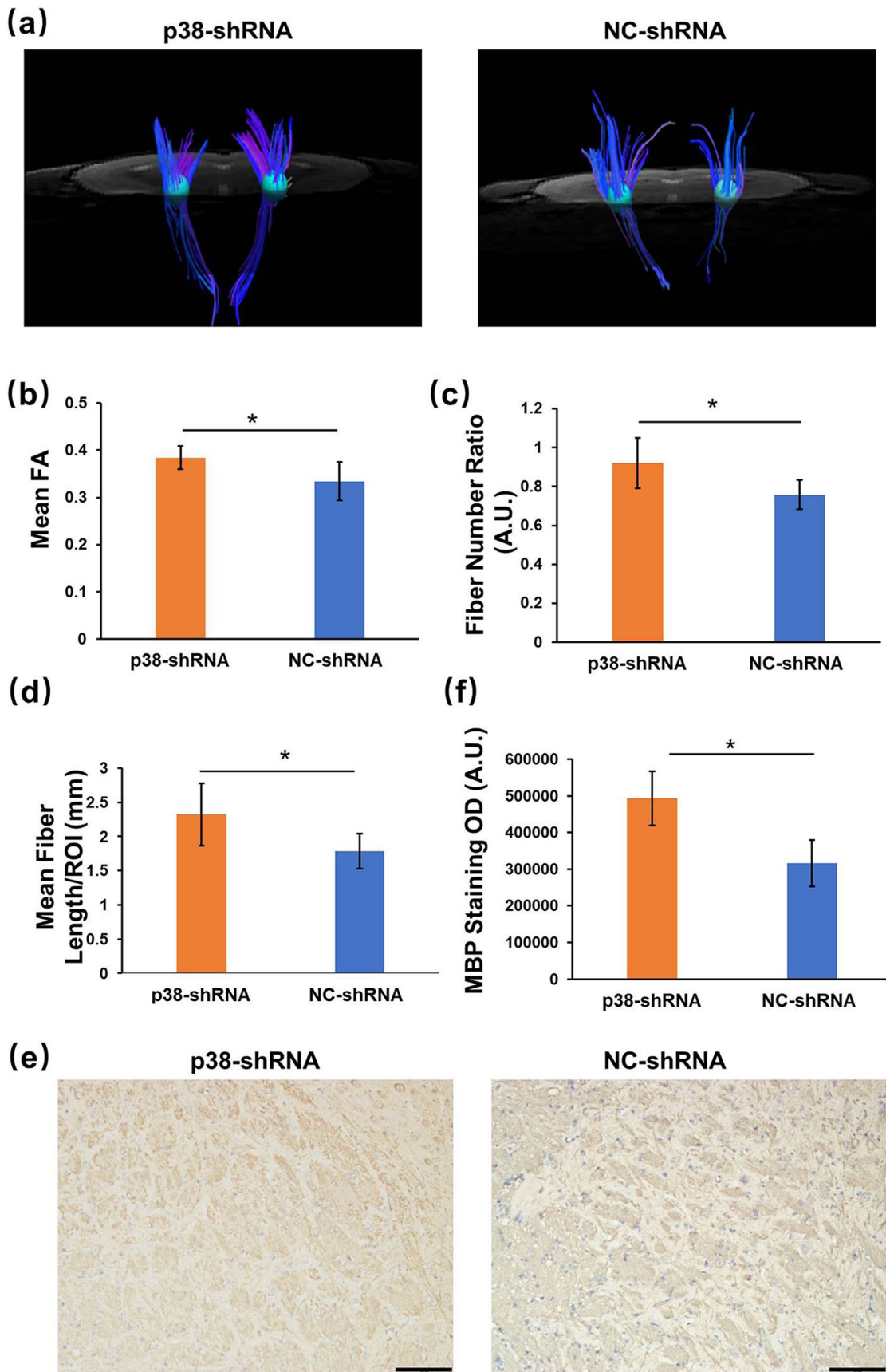Researchers are actively employing new strategies to develop new drugs against cell aging. Candidate drugs are

Figure 5. Mesenchymal stem cells (MSCs) infected with p38 MAPK-shRNA increase axonal remodeling in mice. (a) Diffusion weighted imaging reconstruction showed that the corticospinal tract on the bilateral side. Region of interest was set at the bilateral internal capsule. Quantitative analysis of fractional anisotropy (FA) value (b) and the number (c) and length (d) of fiber tracts in the ipsilateral internal capsule showed significant differences between the two groups. (e) Representative myelin basic protein (MBP) immunohistochemical staining of the ipsilateral internal capsule region are shown (scale bar = 100 μm). (f) Statistical analysis of MBP staining in two groups showed significantly increased number of MBP-positive cells in the ipsilateral internal capsule in the p38-shRNA treated MSCs group. *$P < 0.05$.
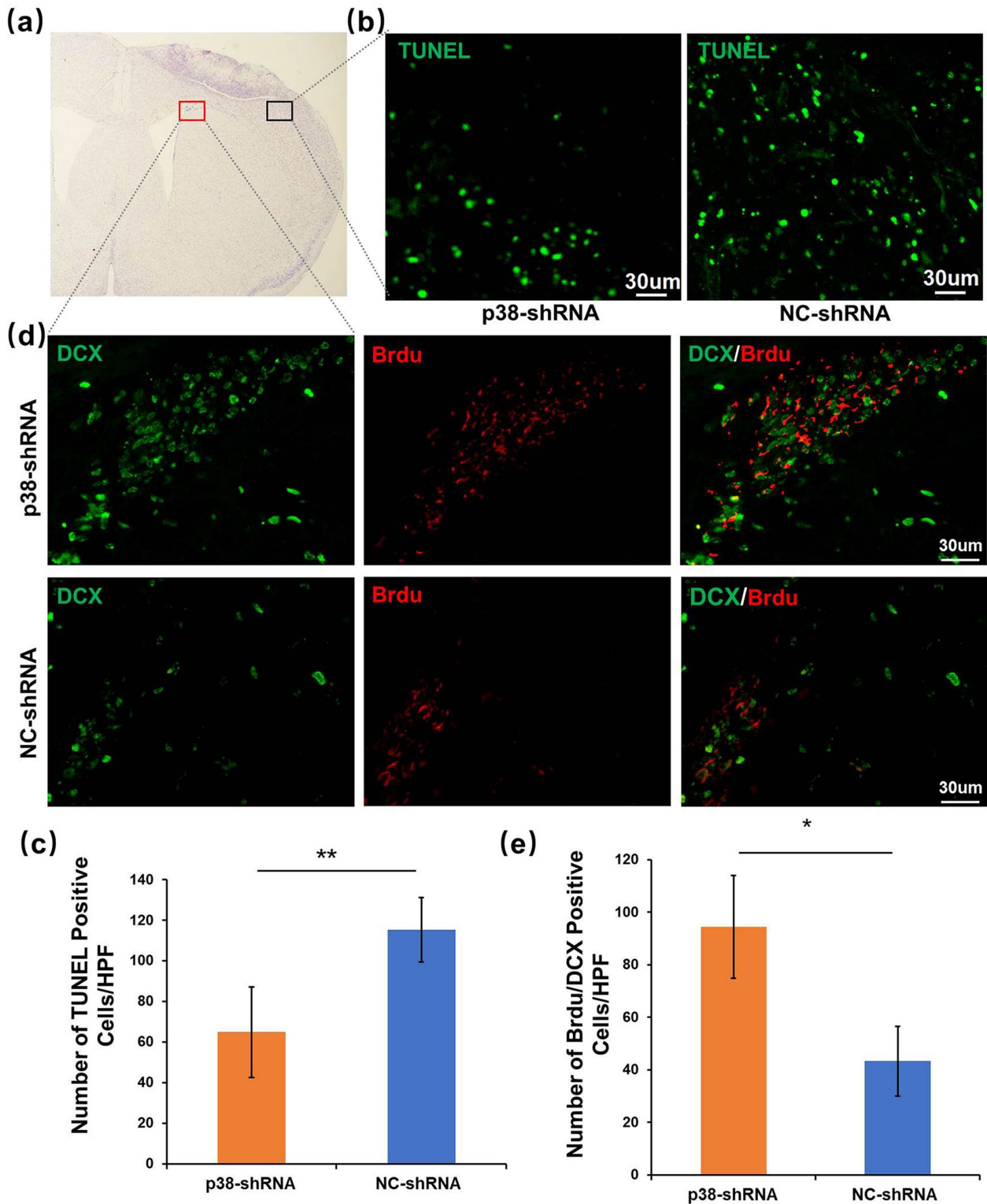
Figure 6. Mesenchymal stem cells (MSCs) infected with p38 MAPK-shRNA promote neurogenesis and decrease apoptosis in mice. (a) Schematic representation of ischemic brain area and sampling areas. TUNEL assay samples are from the area in the black frame, while DCX/Brdu staining samples are from the area in the red frame. (b and c) TUNEL assay indicates decreased cell apoptosis around the ischemia border region in the p38-shRNA group (scale bar = 30 μm). (d and e) Immunofluorescence staining showed more DCX/Brdu double-positive cells in the iplsilateral subventricular zone in the p38-shRNA group than in the control group (scale bar = 30 μm). $*P < 0.05$; $**P < 0.01$.

either senolytic (kill and remove senescent cells) or senomorphic (modify the phenotype of senescent cells to attenuate tissue damage).[23–25] Senomorphic agents include a variety of compounds with different targets and are designed to reduce the senescence-associated secretory phenotype (SASP) and

senescent markers without causing apoptosis.[24] Recent studies have shown that MSCs incubated with tryptophan metabolites produced through the tryptophan hydroxylase (TPH) pathway can resist replicative senescence and cell senescence induced by hyperglycemia or oxidative stress.

It has been reported that 5-methoxytryptophan (5-MTP) can rescue BM-MSCs from high glucose-induced senescence[26] and that melatonin can protect MSCs from replicative and stress-induced senescence.[27] Melatonin and 5-MTP represent a new class of phenotypic compounds that may help protect MSCs against aging and age-related diseases.

The p38 MAPK pathway, which is well known to play an important role in many pathological diseases and in stress-induced cellular senescence, is also a key player in MSC senescence.[28] The CXCR4 signaling pathway in MSCs can reduce oxidative stress[29] and promote osteogenesis[30] and hematopoietic recovery.[29,31] However, with aging, the expression of CXCR4 in MSCs decreases, resulting in MSC dysfunction.[29,31–33] Studies have shown that long-term cultured MSCs induce senescence phenotypes by activating the p38 MAPK signaling pathway and reducing CXCR4 expression, which leads to increased ROS production and increased adipogenesis, as evidenced by the upregulation of *C/EBPa* and *PPARg* gene expression.[34] In contrast, MSCs treated with p38 MAPK inhibitors can avoid premature senescence by increasing CXCR4 expression and reducing oxidative stress, thereby promoting osteogenic differentiation.[34] Because of its role in various physiological activities, such as differentiation, mitosis, survival and apoptosis, p38 MAPK has become a potential therapeutic target for stem cells. The inhibition of p38 MAPK signaling by drugs can reduce the senescence of MSCs[11] and endothelial progenitor cells,[35] enhance the supporting function of MSCs on hematopoietic stem cells,[34] and improve the therapeutic effect of MSCs on myocardial infarction.[36] Our study also confirmed that gene modification based on viral vectors can inhibit p38 MAPK signaling in exogenous MSCs, reduce cell senescence, and thus, improve neurological function, increase axonal remodeling, promote neurogenesis, and decrease neuronal apoptosis in ischemic stroke mice.

The established mouse cranial DTI scanning protocol in this study demonstrated that MSC transplantation in the p38 MAPK-inhibited group led to a significant increase in the number and length of white matter fibers in the ipsilateral internal capsule area after cerebral infarction in mice. DTI is a type of functional MRI that tracks the white matter fibers by describing the anisotropy of water molecule diffusion to assess the integrity and continuity of tissue structure. Tissue structure (membrane, organelles, macromolecules, etc.) and biochemical properties (temperature and viscosity) can fundamentally affect the diffusion of water molecules; therefore, the tissue fiber structure under pathological conditions can affect the diffusion characteristics and anisotropy of water molecules. DTI has been widely used for assessing the central nervous system and plays an important role in the evaluation of ischemic brain diseases, white matter lesions, brain developmental disorders, and the prognosis of brain tumors.[37–39] FA is one of the main parameters used to describe the anisotropy of white matter fibers, is related to the integrity, compactness, and parallelism of the myelin sheath, and can reflect the integrity of white matter fibers.[40] The internal capsule is the most important white matter fiber in brain tissue. The motor nerve axon forms a fiber tract that originates from the ipsilateral cerebral cortex and travels to the contralateral spinal cord after passing through the ipsilateral internal capsule. The results of this study showed that on day 21 after MSC injection, the FA value of the internal capsule on the ipsilateral side was still significantly low, indicating damage to brain white matter fiber tracts and the persistent presence of wallerian degeneration. While, in the p38 MAPK-inhibited group, MSCs promoted an increase in the FA value of the ipsilateral internal capsule after stroke in mice. In addition, *ex vivo* MBP immunohistochemical staining also confirmed that MSC transplantation in the p38 MAPK-inhibited group increased the myelination of nerve fibers in the ipsilateral internal capsule. This gene-based MSC therapy provides a new potential treatment strategy for ischemic stroke and can reduce cell senescence, promote MSC homing, and improve therapeutic efficacy, with broad implications in stem cell biology.

AUTHORS' CONTRIBUTIONS

YB and LW conceptualized the problem. YB and RX developed an experimental method and conducted the experiments. YB and LW did a literature research. YB wrote the manuscript. LW and RX collected resources. LW and YC reviewed and edited. YC supervised the study.

DECLARATION OF CONFLICTING INTERESTS

FUNDING

ORCID IDS

Yingying Bai [ID] https://orcid.org/0000-0002-9312-4314
Ying Cui [ID] https://orcid.org/0000-0003-3954-8228

SUPPLEMENTAL MATERIAL

Supplemental material for this article is available online.

REFERENCES

1. Chung JW, Chang WH, Bang OY, Moon GJ, Kim SJ, Kim SK, Lee JS, Sohn SI, Kim YH, Collaborators S. Efficacy and safety of intravenous mesenchymal stem cells for ischemic stroke. *Neurology* 2021;**96**: e1012–123

2. Dabrowska S, Andrzejewska A, Lukomska B, Janowski M. Neuroinflammation as a target for treatment of stroke using mesenchymal stem cells and extracellular vesicles. *J Neuroinflammation* 2019;**16**:178–95

3. Mani S, Gurusamy N, Ulaganathan T, Paluck AJ, Ramalingam S, Rajasingh J. Therapeutic potentials of stem cell-derived exosomes in cardiovascular diseases. *Exp Biol Med* 2023;**248**:434–44

4. Xu R, Bai Y, Min S, Xu X, Tang T, Ju S. In vivo monitoring and assessment of exogenous mesenchymal stem cell-derived exosomes in mice with ischemic stroke by molecular imaging. *Int J Nanomedicine* 2020;**15**:9011–23

5. Li Q, Zhu Z, Wang C, Cai L, Lu J, Wang Y, Xu J, Su Z, Zheng W, Chen X. CTRP9 ameliorates cellular senescence via PGC1alpha/AMPK signaling in mesenchymal stem cells. *Int J Mol Med* 2018;**42**:1054–63

6. Seeger FH, Haendeler J, Walter DH, Rochwalsky U, Reinhold J, Urbich C, Rossig L, Corbaz A, Chvatchko Y, Zeiher AM, Dimmeler S. p38 mitogen-activated protein kinase downregulates endothelial progenitor cells. *Circulation* 2005;**111**:1184–91

7. Maruyama J, Naguro I, Takeda K, Ichijo H. Stress-activated MAP kinase cascades in cellular senescence. *Curr Med Chem* 2009;**16**:1229–35

8. Kuki S, Imanishi T, Kobayashi K, Matsuo Y, Obana M, Akasaka T. Hyperglycemia accelerated endothelial progenitor cell senescence via the activation of p38 mitogen-activated protein kinase. *Circ J* 2006;**70**:1076–81

9. Feng Z, Deng H, Du J, Chen D, Jiang R, Liang X. Lentiviral-mediated RNAi targeting p38MAPK ameliorates high glucose-induced apoptosis in osteoblast MC3T3-E1 cell line. *Indian J Exp Biol* 2011;**49**:94–104

10. Zhou Y, Liang Y, Wei J, Chen J, Tang Q. Lentiviral-mediated p38 MAPK RNAi attenuates aldosterone-induced myocyte apoptosis. *Mol Med Rep* 2013;**8**:493–8

11. Griukova A, Deryabin P, Sirotkina M, Shatrova A, Nikolsky N, Borodkina A. P38 MAPK inhibition prevents polybrene-induced senescence of human mesenchymal stem cells during viral transduction. *PLoS ONE* 2018;**13**:e0209606

12. Navas TA, Mohindru M, Estes M, Ma JY, Sokol L, Pahanish P, Parmar S, Haghnazari E, Zhou L, Collins R, Kerr I, Nguyen AN, Xu Y, Platanias LC, List AA, Higgins LS, Verma A. Inhibition of overactivated p38 MAPK can restore hematopoiesis in myelodysplastic syndrome progenitors. *Blood* 2006;**108**:4170–7

13. Piao CS, Kim JB, Han PL, Lee JK. Administration of the p38 MAPK inhibitor SB203580 affords brain protection with a wide therapeutic window against focal ischemic insult. *J Neurosci Res* 2003;**73**:537–44

14. Ceulemans AG, Zgavc T, Kooijman R, Hachimi-Idrissi S, Sarre S, Michotte Y. The dual role of the neuroinflammatory response after ischemic stroke: modulatory effects of hypothermia. *J Neuroinflammation* 2010;**7**:74–92

15. Bieber M, Gronewold J, Scharf AC, Schuhmann MK, Langhauser F, Hopp S, Mencl S, Geuss E, Leinweber J, Guthmann J, Doeppner TR, Kleinschnitz C, Stoll G, Kraft P, Hermann DM. Validity and reliability of neurological scores in mice exposed to middle cerebral artery occlusion. *Stroke* 2019;**50**:2875–82

16. Squillaro T, Peluso G, Galderisi U. Clinical trials with mesenchymal stem cells: an update. *Cell Transplant* 2016;**25**:829–48

17. Wu KK. Control of mesenchymal stromal cell senescence by tryptophan metabolites. *Int J Mol Sci* 2021;**22**:697–711

18. Zhou X, Hong Y, Zhang H, Li X. Mesenchymal stem cell senescence and rejuvenation: current status and challenges. *Front Cell Dev Biol* 2020;**8**:364–77

19. Baxter MA, Wynn RF, Jowitt SN, Wraith JE, Fairbairn LJ, Bellantuono I. Study of telomere length reveals rapid aging of human marrow stromal cells following in vitro expansion. *Stem Cells* 2004;**22**:675–82

20. Liu H, Xia X, Li B. Mesenchymal stem cell aging: mechanisms and influences on skeletal and non-skeletal tissues. *Exp Biol Med* 2015;**240**:1099–106

21. Brownlee M. The pathobiology of diabetic complications: a unifying mechanism. *Diabetes* 2005;**54**:1615–25

22. Brownlee M. Biochemistry and molecular cell biology of diabetic complications. *Nature* 2001;**414**:813–20

23. Xu M, Pirtskhalava T, Farr JN, Weigand BM, Palmer AK, Weivoda MM, Inman CL, Ogrodnik MB, Hachfeld CM, Fraser DG, Onken JL, Johnson KO, Verzosa GC, Langhi LGP, Weigl M, Giorgadze N, LeBrasseur NK, Miller JD, Jurk D, Singh RJ, Allison DB, Ejima K, Hubbard GB, Ikeno Y, Cubro H, Garovic VD, Hou X, Weroha SJ, Robbins PD, Niedernhofer LJ, Khosla S, Tchkonia T, Kirkland JL. Senolytics

24. Childs BG, Gluscevic M, Baker DJ, Laberge RM, Marquess D, Dananberg J, van Deursen JM. Senescent cells: an emerging target for diseases of ageing. *Nat Rev Drug Discov* 2017;**16**:718–35

25. Liu J, Ding Y, Liu Z, Liang X. Senescence in mesenchymal stem cells: functional alterations, molecular mechanisms, and rejuvenation strategies. *Front Cell Dev Biol* 2020;**8**:258–75

26. Chang TC, Hsu MF, Shih CY, Wu KK. 5-methoxytryptophan protects MSCs from stress induced premature senescence by upregulating FoxO3a and mTOR. *Sci Rep* 2017;**7**:11133–45

27. Lee JH, Yoon YM, Song KH, Noh H, Lee SH. Melatonin suppresses senescence-derived mitochondrial dysfunction in mesenchymal stem cells via the HSPA1L-mitophagy pathway. *Aging Cell* 2020;**19**:e13111

28. Borodkina A, Shatrova A, Abushik P, Nikolsky N, Burova E. Interaction between ROS dependent DNA damage, mitochondria and p38 MAPK underlies senescence of human adult stem cells. *Aging* 2014;**6**:481–95

29. Singh P, Kacena MA, Orschell CM, Pelus LM. Aging-related reduced expression of CXCR4 on bone marrow mesenchymal stromal cells contributes to hematopoietic stem and progenitor cell defects. *Stem Cell Rev Rep* 2020;**16**:684–92

30. Elmansi AM, Hussein KA, Herrero SM, Periyasamy-Thandavan S, Aguilar-Pérez A, Kondrikova G, Kondrikov D, Eisa NH, Pierce JL, Kaiser H, Ding KH, Walker AL, Jiang X, Bollag WB, Elsalanty M, Zhong Q, Shi XM, Su Y, Johnson M, Hunter M, Reitman C, Volkman BF, Hamrick MW, Isales CM, Fulzele S, McGee-Lawrence ME, Hill WD. Age-related increase of kynurenine enhances miR29b-1-5p to decrease both CXCL12 signaling and the epigenetic enzyme Hdac3 in bone marrow stromal cells. *Bone Rep* 2020;**12**:100270

31. Singh P, Mohammad KS, Pelus LM. CXCR4 expression in the bone marrow microenvironment is required for hematopoietic stem and progenitor cell maintenance and early hematopoietic regeneration after myeloablation. *Stem Cells* 2020;**38**:849–59

32. Li H, Hao L, Li Y, Wang R. Reducing CXCR4 resulted in impairing proliferation and promoting aging. *J Nutr Health Aging* 2018;**22**:785–9

33. Alicka M, Kornicka-Garbowska K, Kucharczyk K, Kepska ö MR, cken M, Marycz K. Age-dependent impairment of adipose-derived stem cells isolated from horses. *Stem Cell Res Ther* 2020;**11**:4–24

34. Budgude P, Kale V, Vaidya A. Pharmacological inhibition of p38 MAPK rejuvenates bone marrow derived-mesenchymal stromal cells and boosts their hematopoietic stem cell-supportive ability. *Stem Cell Rev Rep* 2021;**17**:2210–22

35. Bai YY, Wang L, Chang D, Zhao Z, Lu CQ, Wang G, Ju S. Synergistic effects of transplanted endothelial progenitor cells and RWJ 67657 in diabetic ischemic stroke models. *Stroke* 2015;**46**:1938–46

36. Zhang Z, Zhou S, Mei Z, Zhang M. Inhibition of p38MAPK potentiates mesenchymal stem cell therapy against myocardial infarction injury in rats. *Mol Med Rep* 2017;**16**:3489–93

37. Khalil M, Siddiqui K, Baig A, Shamim MS. Role of diffusion tensor imaging for brain tumour resection. *J Pak Med Assoc* 2022;**72**:1667–9

38. Lope-Piedrafita S. Diffusion tensor imaging (DTI). *Methods Mol Biol* 2018;**1718**:103–16

39. Ciccarelli O, Werring DJ, Wheeler-Kingshott CA, Barker GJ, Parker GJ, Thompson AJ, Miller DH. Investigation of MS normal-appearing brain using diffusion tensor MRI with clinical correlations. *Neurology* 2001;**56**:926–33

40. Shereen A, Nemkul N, Yang D, Adhami F, Dunn RS, Hazen ML, Nakafuku M, Ning G, Lindquist DM, Kuan CY. Ex vivo diffusion tensor imaging and neuropathological correlation in a murine model of hypoxia-ischemia-induced thrombotic stroke. *J Cereb Blood Flow Metab* 2011;**31**:1155–69